Title

Measurement of the branching fraction for $\psi(3686)\to\omega K^+K^-$



Journal

Physical Review D, 89(11)

ISSN

2470-0010

Authors

Ablikim, M

Achasov, MN

Ai, XC

et al.

Publication Date

2014-06-01

DOI

10.1103/physrevd.89.112006

# Measurement of the branching fraction for $\psi(3686) \to \omega K^+ K^-$

M. Ablikim[1], M. N. Achasov[8,a], X. C. Ai[1], O. Albayrak[4], M. Albrecht[3], D. J. Ambrose[41], F. F. An[1], Q. An[42], J. Z. Bai[1], R. Baldini Ferroli[19A], Y. Ban[28], D. W. Bennett[18], J. V. Bennett[18], M. Bertani[19A], J. M. Bian[40], E. Boger[21,f], O. Bondarenko[22], I. Boyko[21], S. Braun[37], R. A. Briere[4], H. Cai[47], X. Cai[1], O. Cakir[36A], A. Calcaterra[19A], G. F. Cao[1], S. A. Cetin[36B], J. F. Chang[1], G. Chelkov[21,b], G. Chen[1], H. S. Chen[1], J. C. Chen[1], M. L. Chen[1], S. J. Chen[26], X. Chen[1], X. R. Chen[23], Y. B. Chen[1], H. P. Cheng[16], X. K. Chu[28], Y. P. Chu[1], D. Cronin-Hennessy[40], H. L. Dai[1], J. P. Dai[1], D. Dedovich[21], Z. Y. Deng[1], A. Denig[20], I. Denysenko[21], M. Destefanis[45A,45C], W. M. Ding[30], Y. Ding[24], C. Dong[27], J. Dong[1], L. Y. Dong[1], M. Y. Dong[1], S. X. Du[49], J. Z. Fan[35], J. Fang[1], S. S. Fang[1], Y. Fang[1], L. Fava[45B,45C], C. Q. Feng[42], C. D. Fu[1], O. Fuks[21,f], Q. Gao[1], Y. Gao[35], C. Geng[42], K. Goetzen[9], W. X. Gong[1], W. Gradl[20], M. Greco[45A,45C], M. H. Gu[1], Y. T. Gu[11], Y. H. Guan[1], L. B. Guo[25], T. Guo[25], Y. P. Guo[20], Z. Haddadi[22], S. Han[47], Y. L. Han[1], F. A. Harris[39], K. L. He[1], M. He[1], Z. Y. He[27], T. Held[3], Y. K. Heng[1], Z. L. Hou[1], C. Hu[25], H. M. Hu[1], J. F. Hu[45A], T. Hu[1], G. M. Huang[5], G. S. Huang[42], H. P. Huang[47], J. S. Huang[14], L. Huang[1], X. T. Huang[30], Y. Huang[26], T. Hussain[44], C. S. Ji[42], Q. Ji[1], Q. P. Ji[27], X. B. Ji[1], X. L. Ji[1], L. L. Jiang[1], L. W. Jiang[47], X. S. Jiang[1], J. B. Jiao[30], Z. Jiao[16], D. P. Jin[1], S. Jin[1], T. Johansson[46], A. Julin[40], N. Kalantar-Nayestanaki[22], X. L. Kang[1], X. S. Kang[27], M. Kavatsyuk[22], B. Kloss[20], B. Kopf[3], M. Kornicer[39], W. Kuehn[37], A. Kupsc[46], W. Lai[1], J. S. Lange[37], M. Lara[18], P. Larin[13], M. Leyhe[3], C. H. Li[1], Cheng Li[42], Cui Li[42], D. Li[17], D. M. Li[49], F. Li[1], G. Li[1], H. B. Li[1], J. C. Li[1], Jin Li[29], K. Li[12], K. Li[30], P. R. Li[38], Q. J. Li[1], T. Li[30], W. D. Li[1], W. G. Li[1], X. L. Li[30], X. N. Li[1], X. Q. Li[27], Z. B. Li[34], H. Liang[42], Y. F. Liang[32], Y. T. Liang[37], D. X. Lin[13], B. J. Liu[1], C. L. Liu[4], C. X. Liu[1], F. H. Liu[31], Fang Liu[1], Feng Liu[5], H. B. Liu[11], H. H. Liu[15], H. M. Liu[1], J. Liu[1], J. P. Liu[47], K. Liu[35], K. Y. Liu[24], P. L. Liu[30], Q. Liu[38], S. B. Liu[42], X. Liu[23], Y. B. Liu[27], Z. A. Liu[1], Zhiqiang Liu[1], Zhiqing Liu[20], H. Loehner[22], X. C. Lou[1,c], G. R. Lu[14], H. J. Lu[16], H. L. Lu[1], J. G. Lu[1], Y. Lu[1], Y. P. Lu[1], C. L. Luo[25], M. X. Luo[48], T. Luo[39], X. L. Luo[1], M. Lv[1], X. R. Lyu[38], F. C. Ma[24], H. L. Ma[1], Q. M. Ma[1], S. Ma[1], T. Ma[1], X. Y. Ma[1], F. E. Maas[13], M. Maggiora[45A,45C], Q. A. Malik[44], Y. J. Mao[28], Z. P. Mao[1], J. G. Messchendorp[22], J. Min[1], T. J. Min[1], R. E. Mitchell[18], X. H. Mo[1], Y. J. Mo[5], H. Moeini[22], C. Morales Morales[13], K. Moriya[18], N. Yu. Muchnoi[8,a], H. Muramatsu[40], Y. Nefedov[21], F. Nerling[13], I. B. Nikolaev[8,a], Z. Ning[1], S. Nisar[7], X. Y. Niu[1], S. L. Olsen[29], Q. Ouyang[1], S. Pacetti[19B], M. Pelizaeus[3], H. P. Peng[42], K. Peters[9], J. L. Ping[25], R. G. Ping[1], R. Poling[40], M. Qi[26], S. Qian[1], C. F. Qiao[38], L. Q. Qin[30], N. Qin[47], X. S. Qin[1], Y. Qin[28], Z. H. Qin[1], J. F. Qiu[1], K. H. Rashid[44], C. F. Redmer[20], M. Ripka[20], G. Rong[1], X. D. Ruan[11], A. Sarantsev[21,d], K. Schoenning[46], S. Schumann[20], W. Shan[28], M. Shao[42], C. P. Shen[2], X. Y. Shen[1], H. Y. Sheng[1], M. R. Shepherd[18], W. M. Song[1], X. Y. Song[1], S. Spataro[45A,45C], B. Spruck[37], G. X. Sun[1], J. F. Sun[14], S. S. Sun[1], Y. J. Sun[42], Y. Z. Sun[1], Z. J. Sun[1], Z. T. Sun[42], C. J. Tang[32], X. Tang[1], I. Tapan[36C], E. H. Thorndike[41], M. Tiemens[22], D. Toth[40], M. Ullrich[37], I. Uman[36B], G. S. Varner[39], B. Wang[27], D. Wang[28], D. Y. Wang[28], K. Wang[1], L. L. Wang[1], L. S. Wang[1], M. Wang[30], P. Wang[1], P. L. Wang[1], Q. J. Wang[1], S. G. Wang[28], W. Wang[1], X. F. Wang[35], Y. D. Wang[19A], Y. F. Wang[1], Y. Q. Wang[20], Z. Wang[1], Z. G. Wang[1], Z. H. Wang[42], Z. Y. Wang[1], D. H. Wei[10], J. B. Wei[28], P. Weidenkaff[20], S. P. Wen[1], M. Werner[37], U. Wiedner[3], M. Wolke[46], L. H. Wu[1], N. Wu[1], Z. Wu[1], L. G. Xia[35], Y. Xia[17], D. Xiao[1], Z. J. Xiao[25], Y. G. Xie[1], Q. L. Xiu[1], G. F. Xu[1], L. Xu[1], Q. J. Xu[12], Q. N. Xu[38], X. P. Xu[33], Z. Xue[1], L. Yan[42], W. B. Yan[42], W. C. Yan[42], Y. H. Yan[17], H. X. Yang[1], L. Yang[47], Y. Yang[5],

Y. X. Yang[10], H. Ye[1], M. Ye[1], M. H. Ye[6], B. X. Yu[1], C. X. Yu[27], H. W. Yu[28], J. S. Yu[23], S. P. Yu[30], C. Z. Yuan[1], W. L. Yuan[26], Y. Yuan[1], A. Yuncu[36B,e], A. A. Zafar[44], A. Zallo[19A], S. L. Zang[26], Y. Zeng[17], B. X. Zhang[1], B. Y. Zhang[1], C. Zhang[26], C. B. Zhang[17], C. C. Zhang[1], D. H. Zhang[1], H. H. Zhang[34], H. Y. Zhang[1], J. J. Zhang[1], J. Q. Zhang[1], J. W. Zhang[1], J. Y. Zhang[1], J. Z. Zhang[1], S. H. Zhang[1], X. J. Zhang[1], X. Y. Zhang[30], Y. Zhang[1], Y. H. Zhang[1], Z. H. Zhang[5], Z. P. Zhang[42], Z. Y. Zhang[47], G. Zhao[1], J. W. Zhao[1], Lei Zhao[42], Ling Zhao[1], M. G. Zhao[27], Q. Zhao[1], Q. W. Zhao[1], S. J. Zhao[49], T. C. Zhao[1], X. H. Zhao[26], Y. B. Zhao[1], Z. G. Zhao[42], A. Zhemchugov[21,f], B. Zheng[43], J. P. Zheng[1], Y. H. Zheng[38], B. Zhong[25], L. Zhou[1], Li Zhou[27], X. Zhou[47], X. K. Zhou[38], X. R. Zhou[42], X. Y. Zhou[1], K. Zhu[1], K. J. Zhu[1], X. L. Zhu[35], Y. C. Zhu[42], Y. S. Zhu[1], Z. A. Zhu[1], J. Zhuang[1], B. S. Zou[1], J. H. Zou[1]

(BESIII Collaboration)

[1] *Institute of High Energy Physics, Beijing 100049, People's Republic of China*
[2] *Beihang University, Beijing 100191, People's Republic of China*
[3] *Bochum Ruhr-University, D-44780 Bochum, Germany*
[4] *Carnegie Mellon University, Pittsburgh, Pennsylvania 15213, USA*
[5] *Central China Normal University, Wuhan 430079, People's Republic of China*
[6] *China Center of Advanced Science and Technology, Beijing 100190, People's Republic of China*
[7] *COMSATS Institute of Information Technology, Lahore, Defence Road, Off Raiwind Road, 54000 Lahore, Pakistan*
[8] *G.I. Budker Institute of Nuclear Physics SB RAS (BINP), Novosibirsk 630090, Russia*
[9] *GSI Helmholtzcentre for Heavy Ion Research GmbH, D-64291 Darmstadt, Germany*
[10] *Guangxi Normal University, Guilin 541004, People's Republic of China*
[11] *GuangXi University, Nanning 530004, People's Republic of China*
[12] *Hangzhou Normal University, Hangzhou 310036, People's Republic of China*
[13] *Helmholtz Institute Mainz, Johann-Joachim-Becher-Weg 45, D-55099 Mainz, Germany*
[14] *Henan Normal University, Xinxiang 453007, People's Republic of China*
[15] *Henan University of Science and Technology, Luoyang 471003, People's Republic of China*
[16] *Huangshan College, Huangshan 245000, People's Republic of China*
[17] *Hunan University, Changsha 410082, People's Republic of China*
[18] *Indiana University, Bloomington, Indiana 47405, USA*
[19] *(A)INFN Laboratori Nazionali di Frascati, I-00044, Frascati, Italy; (B)INFN and University of Perugia, I-06100, Perugia, Italy*
[20] *Johannes Gutenberg University of Mainz, Johann-Joachim-Becher-Weg 45, D-55099 Mainz, Germany*
[21] *Joint Institute for Nuclear Research, 141980 Dubna, Moscow region, Russia*
[22] *KVI, University of Groningen, NL-9747 AA Groningen, The Netherlands*
[23] *Lanzhou University, Lanzhou 730000, People's Republic of China*
[24] *Liaoning University, Shenyang 110036, People's Republic of China*
[25] *Nanjing Normal University, Nanjing 210023, People's Republic of China*
[26] *Nanjing University, Nanjing 210093, People's Republic of China*
[27] *Nankai university, Tianjin 300071, People's Republic of China*
[28] *Peking University, Beijing 100871, People's Republic of China*
[29] *Seoul National University, Seoul, 151-747 Korea*
[30] *Shandong University, Jinan 250100, People's Republic of China*
[31] *Shanxi University, Taiyuan 030006, People's Republic of China*

[32] Sichuan University, Chengdu 610064, People's Republic of China
[33] Soochow University, Suzhou 215006, People's Republic of China
[34] Sun Yat-Sen University, Guangzhou 510275, People's Republic of China
[35] Tsinghua University, Beijing 100084, People's Republic of China
[36] (A)Ankara University, Dogol Caddesi, 06100 Tandogan, Ankara, Turkey; (B)Dogus University, 34722 Istanbul, Turkey; (C)Uludag University, 16059 Bursa, Turkey
[37] Universitaet Giessen, D-35392 Giessen, Germany
[38] University of Chinese Academy of Sciences, Beijing 100049, People's Republic of China
[39] University of Hawaii, Honolulu, Hawaii 96822, USA
[40] University of Minnesota, Minneapolis, Minnesota 55455, USA
[41] University of Rochester, Rochester, New York 14627, USA
[42] University of Science and Technology of China, Hefei 230026, People's Republic of China
[43] University of South China, Hengyang 421001, People's Republic of China
[44] University of the Punjab, Lahore-54590, Pakistan
[45] (A)University of Turin, I-10125, Turin, Italy; (B)University of Eastern Piedmont, I-15121, Alessandria, Italy; (C)INFN, I-10125, Turin, Italy
[46] Uppsala University, Box 516, SE-75120 Uppsala, Sweden
[47] Wuhan University, Wuhan 430072, People's Republic of China
[48] Zhejiang University, Hangzhou 310027, People's Republic of China
[49] Zhengzhou University, Zhengzhou 450001, People's Republic of China

[a] Also at the Novosibirsk State University, Novosibirsk, 630090, Russia
[b] Also at the Moscow Institute of Physics and Technology, Moscow 141700, Russia and at the Functional Electronics Laboratory, Tomsk State University, Tomsk, 634050, Russia
[c] Also at University of Texas at Dallas, Richardson, Texas 75083, USA
[d] Also at the PNPI, Gatchina 188300, Russia
[e] Also at the Moscow Institute of Physics and Technology, Moscow 141700, Russia

(Dated: July 26, 2018version:3)

## Abstract

With $1.06 \times 10^8$ $\psi(3686)$ events collected with the BESIII detector, the branching fraction of $\psi(3686) \to \omega K^+K^-$ is measured to be $(1.54 \pm 0.04 \pm 0.11) \times 10^{-4}$. This is the most precise result to date, due to the largest $\psi(3686)$ sample, improved signal reconstruction efficiency, good simulation of the detector performance, and a more accurate knowledge of the continuum contribution. Using the branching fraction of $J/\psi \to \omega K^+K^-$, the ratio $\mathcal{B}(\psi(3868) \to K^+K^-)/\mathcal{B}(J/\psi \to K^+K^-)$ is determined to be $(18.4 \pm 3.7)\,\%$. This constitutes a significantly improved test of the 12 % rule, with the uncertainty now dominated by the $J/\psi$ branching fraction.

PACS numbers: 14.40.Pq, 13.25.Gv, 13.66.Bc

## I. INTRODUCTION

Since the experimental discovery of the charmonium state $J/\psi$ [1] in 1974, four decades have passed and much experimental and theoretical progress has been achieved. However, puzzles still exist, and the "$\rho\pi$ puzzle" is one of the most famous. From perturbative QCD (pQCD), it is expected that both $J/\psi$ and $\psi(3686)$ decaying into light hadrons are dominated by the annihilation of $c\bar{c}$ into three gluons, with widths proportional to the square of the wave functions at the origin $|\Psi(0)|^2$ [2]. This yields the pQCD "12% rule":

$$Q_h = \frac{\mathcal{B}_{\psi(3686)\to h}}{\mathcal{B}_{J/\psi\to h}} \approx \frac{\mathcal{B}_{\psi(3686)\to e^+e^-}}{\mathcal{B}_{J/\psi\to e^+e^-}} = 12.7\% \ .$$

However, violations of this rule have been found in experiments, and the first and most famous one was observed in the $\rho\pi$ decay mode by Mark II [3], which is now known under the name "$\rho\pi$ puzzle"

Various decay channels have been studied to test the 12% rule, and for different decay modes the experimental ratios can be larger than, smaller than, or consistent with 12%. Many possible mechanisms for the violation of the 12% rule have been proposed, but none of them provide a universally satisfactory explanation at present. A review can be found in Ref. [4]. More experimental studies of the branching fractions of different $J/\psi$ and $\psi(3686)$ decay modes are helpful to understand this puzzle. At present, most measurements consider two-body decays; studies of three- or more-body decays of $J/\psi$ and $\psi(3686)$ will provide complementary information of the decay mechanism and may shed light on the $\rho\pi$ puzzle.

The world average value of the branching fraction for $\psi(3686) \to \omega K^+K^-$ is $(1.85\pm0.25)\times 10^{-4}$ with an error greater than 13% [5]. The world averaged branching fraction of $J/\psi \to \omega K\bar{K}$ [5] is $(1.70\pm0.32)\times10^{-3}$, so $\mathcal{B}(J/\psi \to \omega K^+K^-)$ is determined to be $(0.85\pm0.16)\times10^{-3}$ from isospin symmetry. Then the ratio $Q \equiv \mathcal{B}_{\psi(3686)\to\omega K^+K^-}/\mathcal{B}_{J/\psi\to\omega K^+K^-} = (21.8 \pm 5.0)\%$. While its mean value disagrees with the 12% rule, it is still marginally consistent with 12.7% considering the large uncertainty.

In this paper, we measure the branching fraction of $\psi(3686) \to \omega K^+K^-$ using $1.06 \times 10^8$ $\psi(3686)$ events collected with the BESIII detector at BEPCII; furthermore, 44.49 pb$^{-1}$[6] of $e^+e^-$ data collected at 3.65 GeV is used to determine the continuum contribution. This new and more precise result will be used to determine the ratio $Q$ for this decay channel.

## II. DETECTOR AND MONTE CARLO SIMULATION

The Beijing Electron Positron Collider (BEPCII) [7] is a double-ring $e^+e^-$ collider designed to provide a peak luminosity of $10^{33}$ cm$^{-2}$s$^{-1}$, and the BESIII [7] detector is a general-purpose detector designed to take advantage of this high luminosity. Momenta of charged particles are measured in a 1 T magnetic field with a resolution 0.5% at 1 GeV/c in the helium-based main drift chamber (MDC), and the energy loss ($dE/dx$) is also measured with a resolution better than 6%. The energies and positions of neutral tracks are measured in the electromagnetic calorimeter (EMC) composed of 6240 CsI (Tl) crystals. The energy resolution of 1.0 GeV photons is 2.5% in the barrel and 5.0% in the end-cap regions; the position resolution is 6 mm in the barrel and 9 mm in the end-cap regions. In addition to $dE/dx$, a time-of-flight system (TOF) contributes to particle identification with a time resolution of 80 ps in the barrel and 110 ps in the end-cap regions. The muon system, interspersed in the

steel plates of the magnetic flux return yoke of the solenoid magnet, consists of 1272 $m^2$ of resistive plate chambers (RPCs) in 9 barrel and 8 end-cap layers, which provide a position resolution of 2 cm.

The optimization of the event selection and the estimation of physics backgrounds are performed using Monte Carlo (MC) simulated data samples. The GEANT4-based [8] simulation software BOOST [9] includes the geometric and material description of the BESIII detectors and the detector response and digitization models, as well as the tracking of the detector running conditions and performance. In the MC of inclusive $\psi(3686)$ decays, the production of the $\psi(3686)$ resonance is simulated by the MC event generator KKMC [10]; the known decay modes are generated by BESEVTGEN [11] with branching fractions set at world average values [5], while the remaining unknown decay modes are modeled by LUNDCHARM [12]. In the exclusive MC, the $\psi(3686) \to \omega K^+K^-$ and $\omega \to \pi^+\pi^-\pi^0$ decays are generated with a new data-driven generator based on EvtGen [13].

## III. EVENT SELECTION AND DATA ANALYSIS

Each $\psi(3686) \to \omega K^+K^-$, $\omega \to \pi^+\pi^-\pi^0$ candidate has four good charged tracks with zero net charge and at least two good photon candidates. A good charged track is required to satisfy track fitting, and pass within 10 cm of the interaction point in the beam direction and within 1 cm in the plane perpendicular to the beam. Furthermore, it is required to lie within the angular coverage of the MDC, i.e. $|\cos\theta| < 0.93$ in the laboratory frame, where $\theta$ is the polar angle.

For photon candidates, the shower energy should be greater than 25 MeV in the barrel region and 50 MeV in the end-cap regions, where the barrel is defined as $|\cos\theta| < 0.8$ and the end-cap regions as $0.86 < |\cos\theta| < 0.92$. Also the average time of the hit EMC crystals with respect to the event start time should be between 0 and 700 ns to suppress electronic noise and background hits. The angle between the direction of a photon candidate and any charged track is required to be greater than 20° to avoid showers caused by charged tracks.

The TOF and $dE/dx$ information are combined for each charged track to calculate the particle identification probability ($P_i$ with $i = \pi,\ K$) of each particle type hypothesis. For a pion candidate, $P_\pi > 0.001$ and $P_\pi > P_K$ are required, while for a kaon candidate $P_K > 0.001$ and $P_K > P_\pi$ are required.

A vertex fit is performed assuming all charged tracks are from the IP. A four-constraint (4C) energy- momentum conserving kinematic fit is performed. If there are more than two photon candidates, we loop over all possible combinations, and the combination with the minimum 4C $\chi^2$ is kept for further analysis. The invariant mass of the photon pair is required to be in the range $0.11 < M_{\gamma\gamma} < 0.15$ GeV/$c^2$. Then a 5C kinematic fit is performed with the invariant mass of the two photons constrained to the mass of $\pi^0$, and $\chi^2 < 90$ is required, which is based on the optimization of the figure of merit (FOM), FOM $\equiv N_{sig}/\sqrt{N_{sig}+N_{bg}}$, where $N_{sig}$ and $N_{bg}$ are the numbers of signal and background events estimated by the inclusive MC, respectively.

After all above mentioned selection criteria are applied, the $\pi^+\pi^-\pi^0$ invariant mass distributions of inclusive MC events and data are shown in Fig. 1, in which the points with error bars are data and the histogram is inclusive MC. The inclusive MC sample, which contains the same number of events as the $\psi(3686)$ data and uses the world average $\psi(3686) \to \omega K^+K^-$ branching fraction [5], has more signal events than the data in the region of $0.772 < m_{\pi^+\pi^-\pi^0} < 0.792$ GeV/$c^2$. The selected events with final states $\omega K^+K^-$

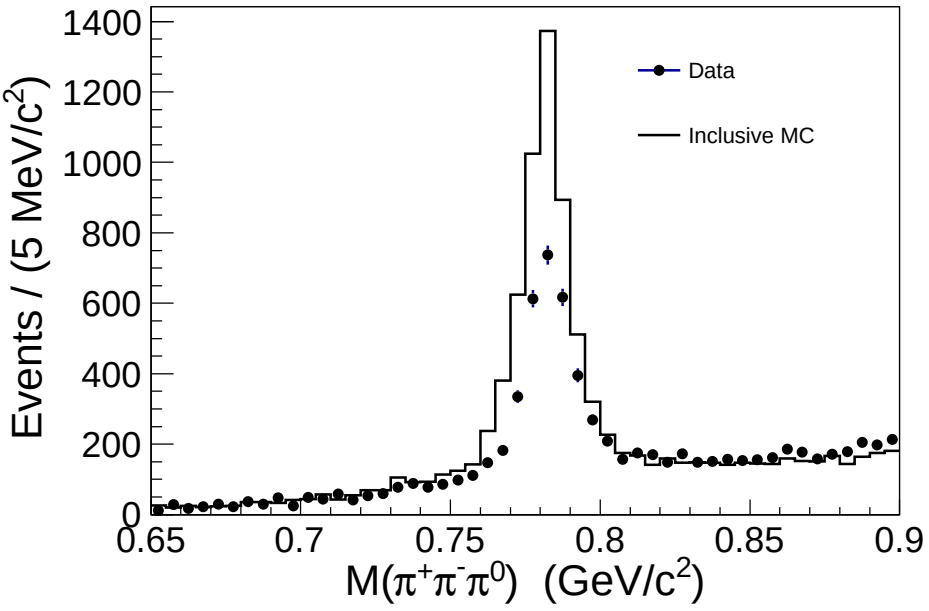


FIG. 1. Comparison of the $\pi^+\pi^-\pi^0$ invariant mass distributions between the inclusive MC simulation and data at 3.686 GeV. The histogram is inclusive MC that is normalized to the luminosity of data, while points with error bars are data.

in the inclusive MC are mainly from three decay channels: $\psi(3686) \to \omega K^+K^-$ (direct), $\psi(3686) \to K_1(1270)K$, $K_1(1270) \to \omega K$ and $\psi(3686) \to \omega f_2(1270)$, $f_2(1270) \to K^+K^-$. And for the distribution of the invariant mass of $\pi^+\pi^-\pi^0$, no peaking background of the $\omega$ signal is found in the fit region ($0.65 < m_{\pi^+\pi^-\pi^0} < 0.9$ GeV/c$^2$). The background simulation from the inclusive MC is reliable as the side-band regions, defined as $0.732 < m_{\pi^+\pi^-\pi^0} < 0.752$ GeV/c$^2$ and $0.812 < m_{\pi^+\pi^-\pi^0} < 0.832$ GeV/c$^2$, match well with data.

Due to the soft transition photon, there is also a possible peaking background from $\psi(3686) \to \gamma\eta_c(2S)$, $\eta_c(2S) \to \omega K^+K^-$, which is not simulated in the inclusive MC sample. It is studied based on an exclusive MC sample of $\psi(3686) \to \gamma\eta_c(2S)$, $\eta_c(2S) \to \omega K^+K^-$ assuming the branching fraction of $\eta_c(2S) \to \omega K^+K^-$ is $10^{-3}$ and taking other branching fractions from the world average value [5]. The contribution from this process is very small, about 0.1% of the observed $\omega K^+K^-$ candidates, and it is ignored.

To determine the signal efficiency, BODY3, a new data-driven generator based on EvtGen [13], is used. BODY3 was developed to simulate contributions from different intermediate states or direct production in data for a given three-body final state. First a MC sample is generated with phase space (PHSP) to determine efficiencies over the whole allowed kinematic region. Next a Dalitz plot and two angular distributions, corrected for efficiency, are used to determine the probability of an event configuration generated randomly by Monte Carlo. For our case, the Dalitz plot of the square of the $\omega K^+$ mass versus the square of the $\omega K^-$ mass and the angular distributions of the $K^+$ and $K^-$ in the $\psi(3686)$ CMS from data are used.

In this analysis there are two three-body decay chains, i.e. $\psi(3686) \to \omega K^+K^-$ and $\omega \to \pi^+\pi^-\pi^0$, so two BODY3 generators are applied in sequence to simulate the whole process. The events in the region of $0.772 < m_{\pi^+\pi^-\pi^0} < 0.792$ GeV/c$^2$ are used to give the

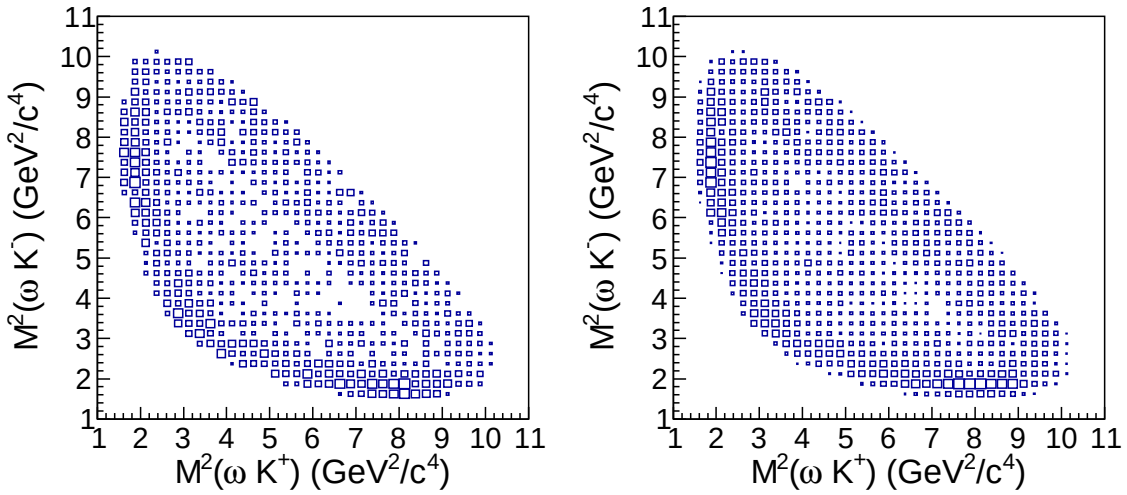


FIG. 2. The Dalitz plots of the data (left) and exclusive MC simulation (right) with the BODY3 generator for events in the region of $0.772 < m_{\pi^+\pi^-\pi^0} < 0.792$ GeV/c$^2$.

probability distribution function as most of $\omega$ candidates are in this region. For the energy points at 3.686 GeV and 3.65 GeV, two different sets of data are used as input to the event generation. Using 3.686 GeV as an example, the comparison between data and MC of Dalitz plots, momentum and angular distributions are displayed in Figs. 2, 3 and 4, respectively. The MC simulation matches the data well in every distribution, so the determination of the signal efficiency should be reliable. While backgrounds have not been subtracted in the BODY3 simulation, their effect will be considered as a systematic uncertainty (see Section IV).

Neglecting possible interference between resonance and non-resonance processes, the $\omega K^+K^-$ yield is obtained by fitting the $m_{\pi^+\pi^-\pi^0}$ distribution. The signal shape is described by a smeared Breit-Wigner function, i.e. BW $\otimes$ Gauss, where the $\sigma$ of the Gaussian describes the resolution and the width of the $\omega$ is fixed at 8.49 MeV/c$^2$ according to the world average value [5]. The background is described by a linear function. For the $\psi(3686)$ data sample, the number of observed signal events is $2781 \pm 68$, and the fit is shown in Fig. 5. From the fit, the mass of $\omega$ is $783.1 \pm 0.2$ MeV/c$^2$, the resolution is $(5.05 \pm 0.28)$ MeV/c$^2$ and the goodness of the fit is $\chi^2/ndf = 107/95 = 1.13$.

A similar event selection and fit method are applied to the 44.49 pb$^{-1}$ $e^+e^-$ data sample collected at 3.65 GeV, in which $100 \pm 11$ signal events are observed, and the fit is shown in Fig. 6. The fit result gives the $\omega$ mass $782.0 \pm 0.9$ MeV/c$^2$, the resolution is $4.4 \pm 1.6$ MeV/c$^2$ and the goodness of fit $\chi^2/ndf = 4.20/4 = 1.05$.

Under the assumption that interference between $\psi(3686)$ decay and continuum production of the same final state is absent, the branching fraction of $\psi(3686) \to \omega K^+K^-$ is determined by the formula

$$\mathcal{B}(\psi(3686) \to \omega K^+K^-) = \frac{N_{3.686}/\epsilon_{3.686} - f_c \cdot N_{3.65}/\epsilon_{3.65}}{\mathcal{B}(\omega \to \pi^0\pi^+\pi^-) \times \mathcal{B}(\pi^0 \to \gamma\gamma) \times N_{\psi(3686)}}\,, \qquad (1)$$

where $\mathcal{B}(\omega \to \pi^0\pi^+\pi^-) = 0.892 \pm 0.007$ is the branching fraction of $\omega \to \pi^+\pi^-\pi^0$ [5], $\mathcal{B}(\pi^0 \to \gamma\gamma) = 0.98823 \pm 0.00034$ is the branching fraction of $\pi^0 \to \gamma\gamma$ [5], $N_{\psi(3686)} =$

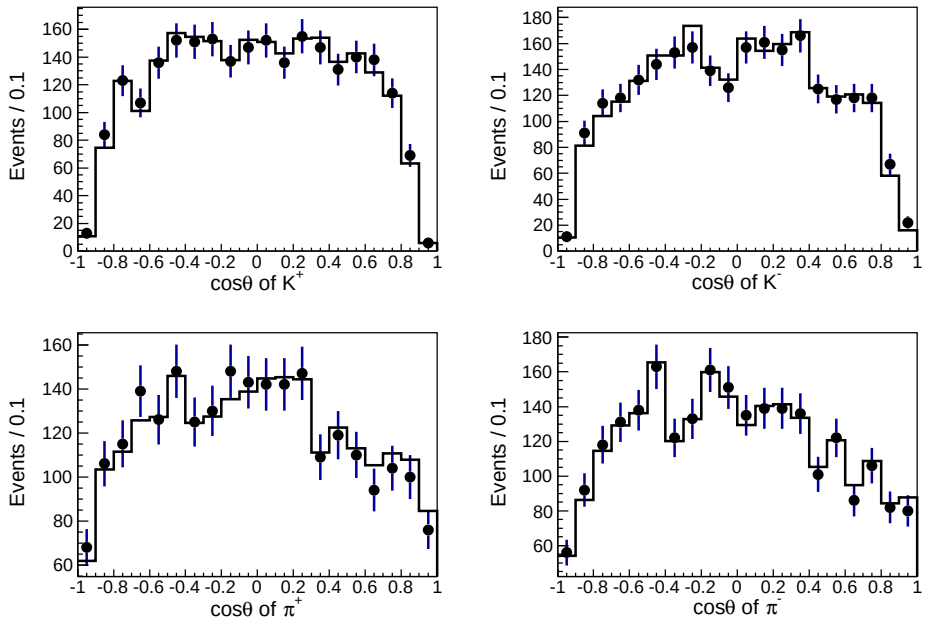


FIG. 3. Comparison of various $\cos\theta$ distributions for $\psi(3686) \to \omega K^+K^-$ candidates of data and signal MC with BODY3 generator for events in the region of $0.772 < m_{\pi^+\pi^-\pi^0} < 0.792$ GeV/c$^2$. The $\cos\theta$ of $K^+$ and $K^-$ is measured in the center-of-mass frame of $\psi(3686)$, and that of $\pi^+$ and $\pi^-$ is of $\omega$. Dots with error bars are data, and the histograms are the signal MC with the BODY3 generators.

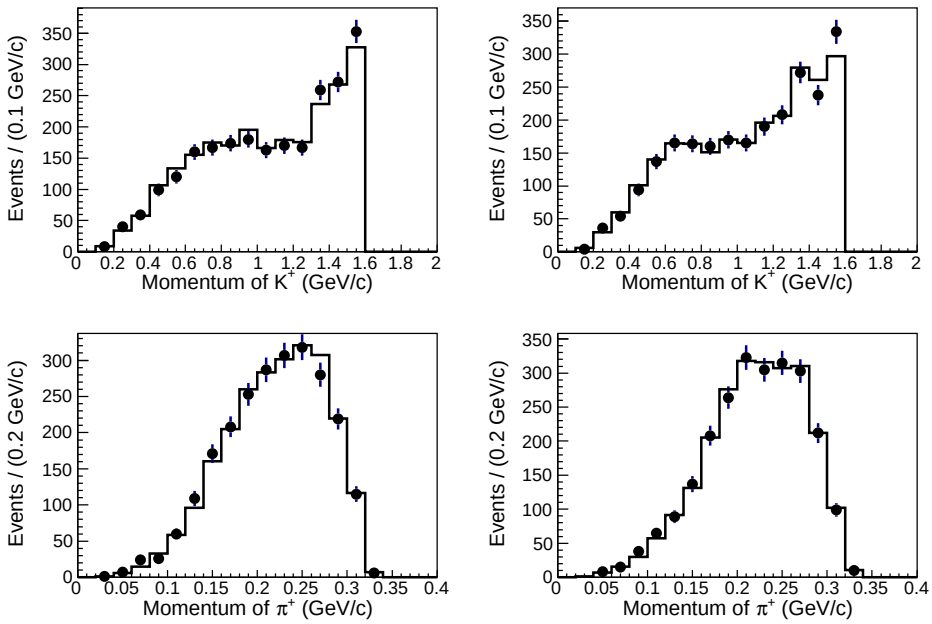


FIG. 4. Comparison of various momentum distributions for $\psi(3686) \to \omega K^+K^-$ candidates of data and signal MC with both BODY3 generator for events in the region of $0.772 < m_{\pi^+\pi^-\pi^0} < 0.792$ GeV/c$^2$. The dots with error bars are data, and the histogram is the signal MC with the BODY3 generators.

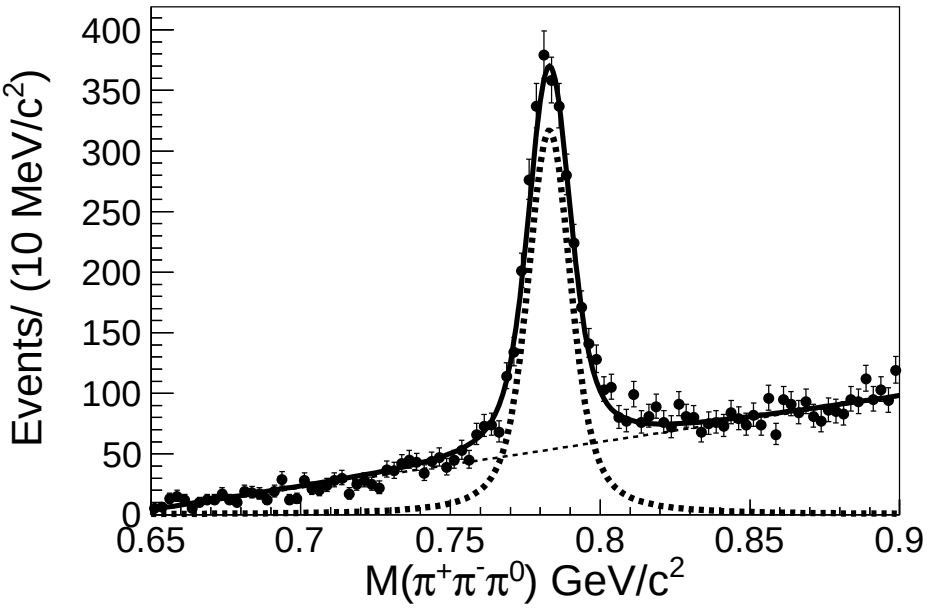


FIG. 5. Fit to data to obtain the yields at 3.686 GeV. The solid line is the total fit result, the dots with error bars are data, the bold dashed line is the signal shape, and the thin dashed line is the background.

$(106.41 \pm 0.86) \times 10^6$ is the number of $\psi(3686)$ events [14], and the scaling factor $f_c = 3.677$ is determined from the luminosities and continuum hadronic cross sections of the two data samples used in this paper [14]. The efficiencies $\epsilon_{3.686} = 16.9\%$ at 3.686 GeV and $\epsilon_{3.65} = 20.7\%$ at 3.65 GeV. $N_{3.686}$ and $N_{3.65}$ are the numbers of events observed in the 3.686 GeV and 3.65 GeV data samples, respectively. Thus $\mathcal{B}(\psi(3686) \to \omega K^+K^-)$ is determined to be $(1.56 \pm 0.04) \times 10^{-4}$, where the uncertainty is only statistical.

## IV. SYSTEMATIC UNCERTAINTIES

The tracking efficiencies of $K$ and $\pi$ have been studied with data samples for the clean processes $J/\psi \to K_S^0 K^\pm \pi^\mp + c.c.$, $K_S^0 \to \pi^+\pi^-$ and $\psi(3686) \to \pi^+\pi^- J/\psi$, $J/\psi \to l^+l^-$, respectively. The difference of charged track efficiencies between data and MC simulated events is 1% per track [15, 16]. Therefore 4% is taken as the total uncertainty in tracking efficiency due to four charged particles in the final states.

The photon reconstruction efficiency has been studied via the processes $J/\psi \to \rho^0\pi^0$, $\rho^0 \to \pi^+\pi^-$, $\pi^0 \to \gamma\gamma$, and 1% is taken as the systematic uncertainty of photon reconstruction [17]. The total systematic uncertainty of photon reconstruction here is 2% since the final states has two photons.

The PID systematic uncertainty is 1% for each charged particle, determined from $J/\psi \to \pi^+\pi^-\pi^0$ and $K^+K^-\pi^0$ [18], so the total PID systematic uncertainty is 4% due to four charged tracks in the final states.

The systematic uncertainty of the kinematic fit is estimated by using the method described in Ref. [16], where helix parameter corrections corresponding to the difference between data and MC is made, and the difference of the efficiencies with and without this

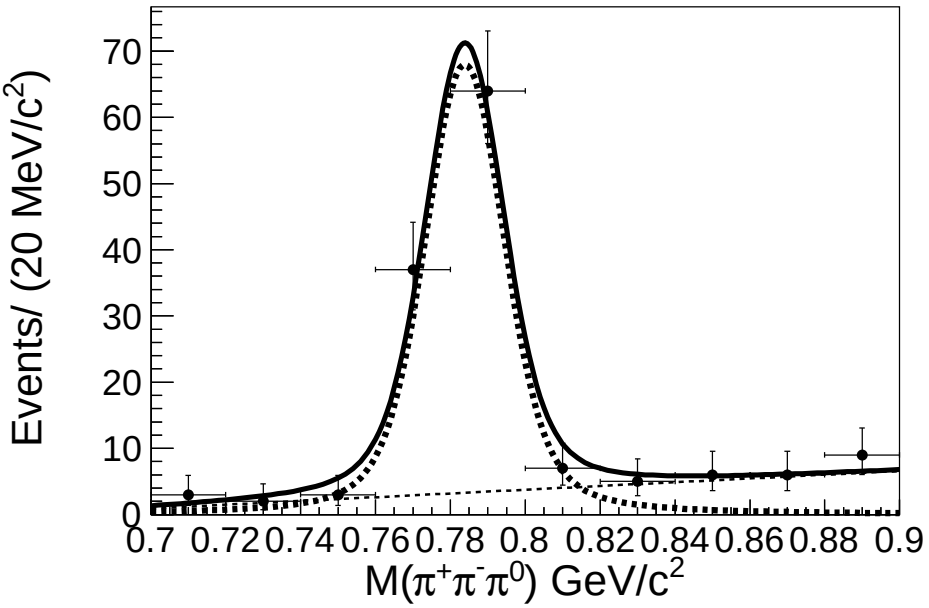


FIG. 6. Fit to 3.65 GeV data to obtain the continuum yield. The solid line is the total fit result, the dots with error bars are data, the bold dashed line is the signal shape, and the thin dashed line is the background.

correction is taken as the systematic uncertainty. In this analysis, the efficiency changes from 17.5% to 17.3% after this correction, so we take 1.1% as the systematic uncertainty of the kinematic fit.

The systematic uncertainty of the background shape is estimated by checking the results with different background shapes, and the maximum difference is quoted as its uncertainty. We used 1st, 2nd and 3rd order polynomial backgrounds, and varied the fit region of $m_{\pi^+\pi^-\pi^0}$ from [0.65 GeV/$c^2$, 0.90 GeV/$c^2$] to [0.60 GeV/$c^2$, 0.95 GeV/$c^2$]. The biggest signal, $2896 \pm 72$, in the 3.686 GeV/$c^2$ data sample is obtained using a second order polynomial background shape and a fit region [0.64 GeV/$c^2$, 0.91 GeV/$c^2$]; the difference with the nominal result yields a 3% systematic uncertainty.

The systematic uncertainty with the BODY3 generator is composed of three parts. The first one is attributed to the limited statistics of the data sample, which is used as input to construct the data simulated by the BODY3 generator. The second one is attributed to the binning method. The third one is from the remaining backgrounds. The first uncertainty is obtained directly. The second one is obtained by varying the binning. The third one is estimated using inclusive MC as input and determining the change of efficiency with and without background . Combining the uncertainties of these three parts, the final uncertainty from the BODY3 generator is 1.3%.

The trigger efficiency is very high due to four charged tracks and two photons in the final states [19], and the systematic uncertainty of the trigger efficiency can be neglected in this analysis.

The number of $\psi(3686)$ events is $(106.41 \pm 0.86) \times 10^6$, which is determined using $\psi(3686) \to$ hadrons [14]. The uncertainty of $f_c$ is small, 0.2% [14], and yields a negligible systematic error on the branching ratio.

The systematic uncertainty of the $\pi^0$ selection is estimated by removing the requirement of 0.11 GeV/c$^2$ $< M_{\gamma\gamma} <$ 0.15 GeV/c$^2$ in event selection. The difference of the result, 0.6% is taken as the systematic uncertainty.

Table I compiles all sources of systematic uncertainties in the measurement of the branching fractions, and the total systematic uncertainty is 7.0%, which is obtained by adding the uncertainties in quadrature.

TABLE I. Summary of systematic uncertainties.

| **Source of uncertainty** | **Uncertainty** |
|---|---|
| MDC tracking | 4.0% |
| PID | 4.0% |
| Photons | 2.0% |
| Kinematic fit | 1.1% |
| Background shape | 3.0% |
| $N_{\psi(3686)}$ | 0.8% |
| $f_c$ | - |
| BODY3 | 1.3% |
| Trigger | - |
| Resolution of $\pi^0$ | 0.6 |
| Total | 7.0% |

## V. SUMMARY

In this paper, the branching fraction of $\psi(3686) \to \omega K^+K^-$ is measured to be $(1.56 \pm 0.04 \pm 0.11) \times 10^{-4}$. The comparison with previous results is displayed in Table II, and our result is the most precise measurement to date. There is a 1.7 $\sigma$ (statistical and systematic) difference between the BESIII and BESII measurements of $\mathcal{B}(\psi(3686) \to \omega K^+K^-)$, and the precision of the BESIII measurement is greatly improved compared to BESII. Part of the improvement is attributed to the determination of the continuum contribution. With the much larger integrated luminosity (44.49 pb$^{-1}$ and 6.4 pb$^{-1}$ for BESIII and BESII) and much higher reconstruction efficiency (20.7% and 2.4% for BESIII and BESII) respectively, the contribution from the continuum process has been determined with much higher precision.

TABLE II. Comparison of our result with previous measurements of the branching fraction $\psi(3686) \to \omega K^+K^-$ and to the world average from particle data group (PDG).

| Branching fraction | Source |
|---|---|
| $(1.56 \pm 0.04 \pm 0.11) \times 10^{-4}$ | this analysis |
| $(2.38 \pm 0.37 \pm 0.29) \times 10^{-4}$ | BESII [20] |
| $(1.9 \pm 0.3 \pm 0.3) \times 10^{-4}$ | CLEO [21] |
| $(1.5 \pm 0.3 \pm 0.2) \times 10^{-4}$ | BES [22] |
| $(1.85 \pm 0.25) \times 10^{-4}$ | PDG [5] |

From the world average value [5], the branching fraction of $J/\psi \to \omega K\bar{K}$ is $(1.70 \pm 0.32) \times 10^{-3}$, and assuming on basis of isospin symmetry that one half is charged kaons, the branching fraction of $J/\psi \to \omega K^+K^-$ is $(0.85 \pm 0.16) \times 10^{-3}$. Therefore, $Q \approx (18.4 \pm 3.7)\%$, which is smaller than the previous result $(21.8 \pm 5.0)\%$ based on the branching ratio of $\psi(3686) \to \omega K\bar{K}$ of the world average value. With the improvement on the measurement of $\psi(3686) \to \omega K^+K^-$, the uncertainty on $Q$ now mainly stems from $J/\psi \to \omega K^+K^-$, and a measurement of the branching fraction of $J/\psi \to \omega K^+K^-$ with at least same precision is needed in order to establish a significant deviation from 12% rule.

## VI. ACKNOWLEDGMENTS

The BESIII collaboration thanks the staff of BEPCII and the computing center for their strong support. This work is supported in part by Joint Funds of the National Natural Science Foundation of China under Contract Nos. U1232109, 11179020; the Ministry of Science and Technology of China under Contract No. 2009CB825200; National Natural Science Foundation of China (NSFC) under Contracts Nos. 10625524, 10821063, 10825524, 10835001, 10935007, 11125525, 11235011, 11079008, 11179007, 11105101, 11205117, 11375221; the Chinese Academy of Sciences (CAS) Large-Scale Scientific Facility Program; CAS under Contracts Nos. KJCX2-YW-N29, KJCX2-YW-N45; 100 Talents Program of CAS; German Research Foundation DFG under Contract No. Collaborative Research Center CRC-1044; Istituto Nazionale di Fisica Nucleare, Italy; Ministry of Development of Turkey under Contract No. DPT2006K-120470; U. S. Department of Energy under Contracts Nos. DE-FG02-04ER41291, DE-FG02-05ER41374, DE-FG02-94ER40823, DESC0010118; U.S. National Science Foundation; University of Groningen (RuG) and the Helmholtzzentrum fuer Schwerionenforschung GmbH (GSI), Darmstadt; WCU Program of National Research Foundation of Korea under Contract No. R32-2008-000-10155-0.

[1] J. J. Aubert *et al.* [E598 Collaboration], Phys. Rev. Lett. **33**, 1404 (1974); J. E. Augustin *et al.* [SLAC-SP-017 Collaboration], Phys. Rev. Lett. **33**, 1406 (1974); G. S. Abrams, D. Briggs, W. Chinowsky, C. E. Friedberg, G. Goldhaber, R. J. Hollebeek, J. A. Kadyk and A. Litke *et al.*, Phys. Rev. Lett. **33**, 1453 (1974).

[2] T. Appelquist and H. D. Politzer, Phys. Rev. Lett. **34**, 43 (1975); A. De Rujula and S. L. Glashow, Phys. Rev. Lett. **34**, 46 (1975).

[3] M. E. B. Franklin, G. J. Feldman, G. S. Abrams, M. S. Alam, C. A. Blocker, A. Blondel, A. Boyarski and M. Breidenbach *et al.*, Phys. Rev. Lett. **51**, 963 (1983).

[4] D. M. Asner, T. Barnes, J. M. Bian, I. I. Bigi, N. Brambilla, I. R. Boyko, V. Bytev and K. T. Chao *et al.*, Int. J. Mod. Phys. A **24**, S1 (2009)

[5] J. Beringer *et al.* [Particle Data Group Collaboration], Phys. Rev. D **86**, 010001 (2012).

[6] M. Ablikim *et al.* [BESIII Collaboration], Chin. Phys. C **37**, 123001 (2013)

[7] M. Ablikim *et al.* [BESIII Collaboration], Nucl. Instrum. Meth. A **614**, 345 (2010)

[8] S. Agostinelli *et al.* [GEANT4 Collaboration], Nucl. Instrum. Meth. A **506**, 250 (2003).

[9] Z. Y. Deng *et al.* [BESIII Collaboration], High Energy Phys. Nucl. Phys. **30**, 371 (2006).

[10] S. Jadach, B. F. L. Ward and Z. Was, Comput. Phys. Commun. **130**, 260 (2000) S. Jadach, B. F. L. Ward and Z. Was, Phys. Rev. D **63**, 113009 (2001)

[11] R. -G. Ping, Chin. Phys. C **32**, 599 (2008).
[12] J. C. Chen, G. S. Huang, X. R. Qi, D. H. Zhang and Y. S. Zhu, Phys. Rev. D **62**, 034003 (2000).
[13] D. J. Lange, Nucl. Instrum. Meth. A **462**,152 (2001).
[14] M. Ablikim *et al.* [BESIII Collaboration], Chin. Phys. C **37**, 063001 (2013)
[15] M. Ablikim *et al.* [BESIII Collaboration], Phys. Rev. D **87**, 052005 (2013)
[16] M. Ablikim *et al.* [BESIII Collaboration], Phys. Rev. D **87**, 012002 (2013)
[17] M. Ablikim *et al.* [BESIII Collaboration], Phys. Rev. D **81**, 052005 (2010)
[18] M. Ablikim *et al.* [BESIII Collaboration], Phys. Rev. D **83**, 112005 (2011)
[19] N. Berger, K. Zhu, Z. -A. Liu, D. -P. Jin, H. Xu, W. -X. Gong, K. Wang and G. -F. Cao, Chin. Phys. C **34**, 1779 (2010)
[20] M. Ablikim *et al.* [BES Collaboration], Phys. Rev. D **73**, 052004 (2006)
[21] R. A. Briere *et al.* [CLEO Collaboration], Phys. Rev. Lett. **95**, 062001 (2005)
[22] J. Z. Bai *et al.* [BES Collaboration], Phys. Rev. D **67**, 052002 (2003)